

## **Development and examination of high-performance fluidised-bed vibration drier for processing food production waste**

H. Kaletnik<sup>1</sup>, I. Sevostianov<sup>1</sup>, V. Bulgakov<sup>2</sup>, I. Holovach<sup>2</sup>, V. Melnik<sup>3</sup>,  
Ye. Ihnatiev<sup>4</sup> and J. Olt<sup>5,\*</sup>

<sup>1</sup>Vinnitsia National Agrarian University of Ukraine, 3 Soniachna Str., UA21008 Vinnitsia, Ukraine

<sup>2</sup>National University of Life and Environmental Sciences of Ukraine, 15 Heroyiv Oborony Str., UA03041 Kyiv, Ukraine

<sup>3</sup>Kharkiv Petro Vasylenko National Technical University of Agriculture, 44 Alchevskih Str., Kharkiv, UA61002, Ukraine

<sup>4</sup>Dmytro Motornyi Tavria State Agrotechnological University, 18B, Khmelnytsky Ave, UA72310 Melitopol, Zaporozhye Region, Ukraine

<sup>5</sup>Estonian University of Life Sciences, Institute of Technology, 56 Kreutzwaldi Str., EE51006 Tartu, Estonia

\*Correspondence: [jyri.olt@emu.ee](mailto:jyri.olt@emu.ee)

**Abstract.** Drying and processing wet particulate food production waste, such as distillery dreg, brewer's grains, beet pulp, spent coffee and barley slurry etc. for their further use as cattle fodder or fuel is an important and topical problem, which needs effective solutions. As a solution of the problem, the authors have developed improved equipment and a fluidised bed vibration drier, which ensures reaching the required output of the work process and final moisture content in the waste at a minimum power and material intensity and features the combination of the high feasibility with the high reliability of design. In order to validate the improved drying work process together with the optimum parameters of the vibration drier, theoretical investigations based on the mathematical model of the process developed by the authors have been carried out. The process of the vibration drier's frame oscillating together with the waste has been examined, which has resulted in the generation of the differential equation that analytically describes the said process. The work process under consideration has been researched into from the thermophysical point of view using the specific initial data typical for the specific food producer. The research has resulted in obtaining the following design and process parameters of the vibration drier, in particular, for its heating pipes: diameter  $r_t = 0.1$  m; length  $l_t = 5$  m; number  $n_t = 20$ , heat-transfer factor  $K_p = 30$  and the final temperature of the dried food production waste  $t_{o2} = 80$  °C. The listed parameters provide for reaching the required final moisture content in the dried food production waste. Also, new relations have been generated for determining the principal process parameters of the improved drier (productive capacity, heat consumption, mass of heat carrier, waste conveyance speed, sizes and masses of the drier's actuating elements). The obtained relations can be applied in the further theoretical and experimental research on the drier as well as the development of standard methods for its design and calculation.

**Key words:** drying, fluidized bed drier, mathematical modeling, moisture, reactor, vibration, waste.

## INTRODUCTION

In the food producing companies of Ukraine and a number of other countries, the by-products generated as a result of food production, such as distillery dreg, brewer's grains, beet pulp, spent coffee and barley slurry, are mostly dumped to specially allocated landfills, which results in environmental pollution. Processing such waste in order to produce either biological fodder supplements or fuel requires considerable investment and operating costs (Filonenko & Grishin, 1971; Sevastianov, 2013; Ma et al., 2018; Kliuchnikov, 2019). In European countries and the US, such processing is generally implemented in the form of water removal in decanter centrifuges (McKenna, 1986; Beránek & Kolařík, 2014; Altieri et al., 2020), dehydrating in vacuum driers or with the use of bioreactors (Atkinson & Mavituna, 1991; Tribuzi & Laurindo, 2014; Antal, et al., 2015). That said, the mechanical water removal with the use of the most common equipment, such as screw presses and decanter centrifuges, is unable to deliver a final moisture content of less than 74–76% in the processed waste, which implies need in its additional drying prior to using it as animal fodder or fuel and results in the considerable increase of the total power consumption rate of the work process (Panfilov et al., 2001; Sevostianov, 2013). With regard to biological reactors, it has to be noted that they are rather complex and bulky process systems, too expensive for the majority of the national food and processing industry companies. In the papers (Boyce, 1965; Bruce & Giner, 1993; Filonenko & Grishin, 1971; Hemis, et al, 2012; Giner, 2019), the high efficiency of the vibration impact water removal from the above-mentioned food by-products in process units with hydraulic-pulse drives is proved theoretically and experimentally. That technique ensures reducing the final moisture content in the food production waste from the initial value of  $U_{n.o} = 90\text{--}95\%$  to  $U_{k.o} = 20\text{--}25\%$  (moisture content after dehydration), the energy intensity of the process staying at about  $7 \text{ (kW h) t}^{-1}$  and a daily output reaching up to 1900 t of dehydrated waste (Sevostianov, 2013; Sevostianov et al., 2015). Nevertheless, even when applying the latter technique, the dehydrated waste still needs to be additionally dried to a moisture content level of about  $U_{c.o} = 8\%$  in order to provide for its long-term storage (Atkinson, 1979).

In view of the above-stated circumstances, it is a topical problem to improve the methods and equipment used for drying food production waste in order to provide it with the necessary properties at the minimum energy intensity and the targeted production rate.

According to the results of the investigations presented in a number of papers, the air-fluidised and vibration-fluidised bed apparatus are among the most efficient types of driers. In comparison with the drum, tunnel, tower, continuous-belt and roll driers, they maintain a continuous and higher-output work process, in which the targeted values of the final moisture content in the processed material are achieved (Sazhin, 1984; Daud, 2008; Ovchinnikov et al., 2009; Aboltins & Upits, 2012; Bulgakov et al., 2018). The air-fluidised bed and vibration-fluidised bed apparatus include atomizing (spray), convection, vibrating (shaker), spiral, cyclone and flash driers as well as pneumatic pipe driers (Filonenko & Grishin, 1971; Mujumdar, 2014).

In the paper (Ostrikov et al, 2006), various designs of atomizing driers are presented: with central involute heat carrier supply (direct-flow); with central heat carrier supply and separate removal of the gas and the product; with uniform distribution of the supplied gas over the cross-section via a gas-distributing grill; with radial (peripheral) heat carrier supply and central exhaust. The listed equipment delivers a sufficiently high

productive capacity of the work process, but features a rather high energy intensity due to the fact that the motion of waste particles in the operating space is created with the use of the most energy-intensive method of pneumatic transport (design velocity of material particles is  $6\text{--}12\text{ m s}^{-1}$ ), while the removal of water from them is achieved by burning expensive organic heat carriers (Ostrikov et al., 2006). Moreover, its shortcomings include the frequent clogging of the pneumatic nozzles in the driers as well as their rapid abrasive wear (Sazhin, 1984).

During the operation of vibration driers (El Hor et al., 2005; Palamarchuk et al., 2018; Bulgakov et al., 2020), the material in the process chamber passes, as a result of the latter's oscillations, into the state of the fluidised bed or the vibratory fluidised bed (Goncharevich, 1977; Handayani et al., 2017; Hoffman et al., 2017; Lehmann et al., 2019), in which the particles mutually depart from each other, get thoroughly mixed, the heat carrier efficiently enters the space between particles and carries away the moisture. This type of the equipment under consideration is, in the authors' opinion, the most promising one, as it delivers the required values of the final moisture content  $U_{c.o} = 8\%$  with the minimum consumption of energy and time. However, the above equipment has a disadvantage of the complex and material-intensive design. Another drawback is that the majority of industrial vibration driers falls into the category of batch-type equipment, which implies great amounts of time being spent for the batch loading and unloading operations, while these operations are performed with the assistance of auxiliary machines outside the main process cycle, and that has a negative impact on the productivity of the process.

Also, (Panfilov et al., 2001; Wang, et al., 2011; Yogendrasasidhar & Setty, 2019) contains several designs of pneumatic driers, in which the fluidised or vibratory fluidised bed is created with the use of hot heat carrier streams passing through the material pulverized by a rotating disk: pneumatic transport with additional intensive heating (see the note above). The dispersal process alone consumes  $50\text{--}60\text{ kW}$  per ton of pulverized material (Ostrikov et al., 2006). The gaseous heat carrier flow rate is  $8,000\text{ m}^3\text{ h}^{-1}$  (Sazhin, 1984). Another drawback is the high possibility of the disk holes being clogged with particles of the material. Even lower expectations are with regard to the pneumatic driers, in which the processed material is transported in a continuous flow along the bearing surface of the process chamber. In these driers, the heat carrier is fed through the holes in the bearing surface, passes through the bed of the material bringing it into the fluidised or vibratory fluidised state (Mohseni et al., 2019).

The spray drier presented in (Panfilov et al., 2001; Ostrikov et al., 2006; Robaina-Mesa & Chanfrau, 2019; Wawrzyniak et al., 2020) in which mixed flows of the processed material and the heat carrier are used, features considerable design complexity, a high material intensity and large dimensions (unit comprises up to 20 separate apparatus), while the spraying requires the supply of pressure at a level of  $10\text{--}20\text{ MPa}$  (Ostrikov et al., 2006). It is worth mentioning that the auxiliary equipment used for preparing the heat carrier, removing processed material particles from it and separating the liquid and gaseous phases of the used heat carrier is also employed in the other apparatus analysed earlier in this paper.

The driers discussed in the paper (Dufour, 2006), that is, the driers with spiral channels, through which the mixture of the processed material and the heat carrier passes, cyclone driers and two-stage pipe drier installations have specific areas of application and high energy consumption (drying medium flow rate -  $12,000\text{--}15,000\text{ m}^3\text{ h}^{-1}$ ), while

the two latter types - large dimensions as well.

Moreover, the power input required for the removal of water from the waste under consideration with the use of the known designs of rotary drum driers amounts to about 2,500 kW h per ton of removed liquid, spray driers - 2,250 kW h t<sup>-1</sup>, double-drum driers - 1,300 kW h t<sup>-1</sup>, vacuum dryers - 740–760 kW h t<sup>-1</sup>. The listed figures indicate that the energy consumption rates in the work processes of food production waste drying with the use of the known designs of driers are very high and, consequently, have to be reduced.

Overall, the analysis that has been carried out by the authors has brought them to a conclusion that the currently known drying machinery used in integrated process facilities for the recovery of food production waste needs improvement in the direction of cutting down the power intensity of the work process, reducing the dimensions and increasing the operational reliability of the equipment.

The aim of this research is to provide for achieving the minimum power intensity of the work process, in which the food production waste is dried for its further recycling, by means of developing a new design of the vibration drier with a fluidised bed and also theoretically and experimentally proving its rational design and process parameters.

## MATERIALS AND METHODS

For the purpose of developing a high-efficiency vibration drier with fluidised bed and analysing its properties, the authors have applied the methods of comparison, criterion scores and optimisation, the principles and relations of the theoretical mechanics, fluid mechanics, heat engineering, the theory of food production process and apparatus engineering as well as the theory of vibration and vibratory percussion equipment.

The authors have developed a new fluidised bed drier, which provides for efficiently drying food production waste in batches.

In Fig. 1, the design and process schematic model is presented for the new vibration drier designed for processing food production waste. The work process of food production waste drying takes place as follows. The waste is fed into the drier under consideration immediately after its preliminary four-stage mechanical dehydration in the unit described in (Ward, 2002; Ruiz Celma et al., 2012; Sevostianov & Luchik, 2017), after

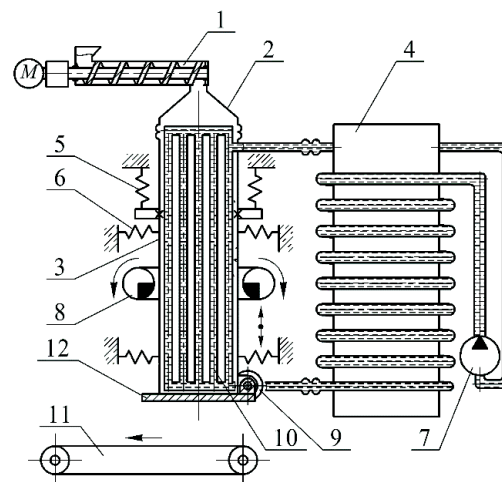


**Figure 1.** Design and process schematic model of vibration drier for processing food production waste: 1 – auger feeder; 2 – conical top; 3 – casing shell, 4 – heat exchanger on process tank of primary production process; 5 – vertical springs; 6 – horizontal springs; 7 – heat exchanger pump; 8 – unbalance vibration exciter; 9 – electric motor; 10 – heating pipes; 11 – belt conveyor; 12 – discharge slide valve.

which its moisture content does not exceed the earlier indicated target value of  $U_{k.o} = 20\text{--}25\%$  (Sevostianov & Luchik, 2017). In the process of feeding, the casing shell of the drying apparatus is filled with food by-products by the auger feeder 1, the slide valve 12 being closed.

The process of feeding the waste into the vibration drier's in casing shell 3 continues until the pressure transducer installed on the inner surface of the slide valve 12 sends the signal that activates the respective relay switch, after which the auger feeder 1 stops operating. The heating pipes 10 form a rigid structure, which is connected via bellow rubber tubes to the heat exchanger on the process tank 4. The circulation of the heat carrier along the pipes 10 and the pipe coil is maintained by the pneumatic or hydraulic pump 7, hence, the preparation of the heat carrier for food production waste drying is performed virtually without any energy input. The direction of the heat carrier flow supplied by the pump 7 and guided into the pipes 10 is shown with the arrows. The heat energy is transferred from the pipes 10 to the batch of food production waste fed into the spaces between them, which ensures the efficient removal of the liquid phase as in the peripheral, so in the middle layers of the batch. Moreover, in order to intensify the drying process, the shell 3 with the food by-products is set in oscillatory motion with the use of the unbalance vibration exciters 8. For that purpose, the casing shell 3 is suspended on vertical springs 5 and horizontal springs 6, while its freedom of movement with respect to the auger feeder 1 is facilitated with the use of a bellow rubber pipe.

Due to the oscillatory motion of the casing shell 3, the particles of the food production waste batch inside the shell 3 become vibration-fluidised, which facilitates more active and less energy-intensive removal of the liquid phase from them. The said phase escapes outside the shell through the small holes in the walls of the casing shell 3 covered inside by filter gauze (not shown in the schematic model). When the electronic moisture meter senses that the pre-set value  $U_{c.o} = 8\%$  of the final moisture content in the food production waste batch in the casing shell is reached, it sends the command signal that starts the stepping motors 9, which turn and open the slide valves 12. The batch of dehydrated food by-products is poured out onto the conveyor belt 11, then the slide valves 12 are again closed and the auger feeder 1 is started. The casing shell 3 is filled with a new batch of food production waste and the next drying cycle begins.

Depending on the type of waste, its initial moisture content at the drier's inlet equal to  $U_{k.o} = 20 - 25\%$  and the temperature of the heat carrier in the pipes, in some instances the continuous mode of operation can be established, when the food production waste continuously passes through the casing shell 3 obtaining in this process the pre-set final moisture content of  $U_{c.o} = 8\%$ . For that purpose, by means of experiments with turning the slide valves 12, the area of the bottom passage in the casing shell is adjusted to the required size, which governs the time of the waste staying inside the shell.

### VIBRATION DRIER MODEL

The advantages of the proposed vibration drier in comparison with the other earlier described equipment for drying with the use of the air-fluidised and vibration-fluidised bed are: the simplicity and compactness of its design, multipurpose application, absence of the danger of clogging the passage spaces in the casing shell, the efficient transfer of heat to the particles of the material throughout the whole cross-section of the shell, the simplicity and fail-safety of the auxiliary heat carrier preparation equipment, the absent

need for cleaning the heat carrier and separating it into phases and the most important feature - the minimum input of energy for the drying process itself due to the utilisation of the heat output from the primary process.

It is necessary to analyse the principal efficiency parameters of the vibration drier operation and establish their relations with the operation and design parameters of the equipment under investigation as well as the physical and mechanical properties of the processed waste.

In order to ensure that the particles of the processed batch of food production waste situated in the casing shell of the vibration drier pass into the vibration-fluidised state, it is necessary to meet the following condition (Bezbakh & Bakhmutyan, 2006):

$$\ddot{x} \geq (2 \div 3)g, \quad (1)$$

where  $\ddot{x}$  – acceleration in the oscillatory motion performed by the vibration drier casing shell;  $g$  – acceleration of gravity.

The acceleration in the oscillatory motion of the vibration drier casing shell specified by (1) can be determined basing on the generation of a mathematical model for the shell's oscillations in the longitudinal and vertical plane. Within the framework of the said mathematical model, it is necessary to generate the differential equation of the vertical translational oscillations performed by the vibration drier casing shell suspended on the springs during the operation of the drier's unbalance vibration exciter, in order to obtain the relation between the above-mentioned acceleration and the design and kinematic parameters of the vibration drier under consideration.

For the development of the mathematical model, i.e. to obtain the required differential equation of motion for the vibration drier casing shell, it is necessary, first of all, to generate the equivalent schematic model.

In this process, the following tentative assumptions are made. First of all, the elastic forces generated by the bellow pipes that connect the vibration drier casing shell and the auger feeder are disregarded as negligible. Moreover, taking into account the fact that the eccentric weights of the vibration exciter have identical geometric and dynamic parameters, but rotate with mutually opposite senses, the oscillations of the vibration drier casing shell in the horizontal plane can be neglected. The above-mentioned equivalent schematic model is shown in Fig. 2.

In this instance, the vibration drier casing shell is considered in the form of a separate body mounted in the frame on several springs and capable of moving in the vertical plane up and down during the operation of the vibration exciters rigidly attached to it. In Fig. 2, the vibration drier casing shell is shown in the position at the random instant of time  $t$  during its translational vertical oscillation. It can be assumed that the vibration drier casing shell is shown in the equivalent schematic model in its uppermost position. In the equivalent schematic model, the vertical axis  $x$  is designated, which is aligned with the longitudinal symmetry axis of the casing shell and has its origin at the point  $O$  that coincides with the bottom end of the casing shell, when the latter is in its equilibrium position. Thus, it is assumed that the vibration drier's casing shell is in its equilibrium position, when its side springs  $D_i L_i$  ( $i = \overline{1,4}$ ) on both sides of it are aligned horizontally (that is, the points of attachment  $L_3, D_3, L_4$  and  $D_4$  of the lower lateral springs  $L_3 D_3$  and  $L_4 D_4$  are level with the point  $O$  to an accuracy of the static deformation of the said springs). Accordingly, when the vibration drier casing shell moves up or down from its equilibrium position, all the lateral springs  $D_i L_i$  ( $i = \overline{1,4}$ ) expand, then, when the casing

shell moves back to the equilibrium position, they contract. The lateral spring attachment points  $L_1, L_2, L_3$  and  $L_4$  are situated on the frame.

Since the point  $O$  is designated as the origin of the  $Ox$  one-dimensional coordinate system, it can be stated that the vibration drier casing shell performs translational vertical oscillations along the above-mentioned axis.

In view of that, the position of the vibration drier casing shell at the random instant of time  $t$  is specified by the coordinate  $x$  that shows the displacement of the casing shell from the equilibrium position. In Fig. 2 the case is shown, when the vibration drier casing shell is situated at the position that is higher than the equilibrium position exactly by the  $x$  value. In this instance,  $0 \leq x \leq x_{max}$ , where  $x_{max}$  – amplitude of oscillations performed by the vibration drier casing shell. In the cases, when the vibration drier casing shell is situated below the equilibrium position, the following condition takes place:  $-x_{max} \leq x \leq 0$ .

The vertical springs  $A_1B_1$  and  $A_2B_2$  ( $A_1, A_2$  and  $B_1, B_2$  – points of attachment of the vertical springs to the frame and the vibration drier casing shell, respectively) contract, when the casing shell moves up, during its down movement they expand. The maximum magnitude of their deformation is equal to two amplitudes of the casing shell oscillations, that is  $2x_{max}$ . The stiffness factors of the springs are assigned the following designations:  $C_{vi}$  ( $i = \overline{1,2}$ ) for vertical and  $C_{hi}$  ( $i = \overline{1,4}$ ) for horizontal springs.

Hence, the elastic forces generated by all the above-mentioned springs are restoring forces in the oscillatory process under consideration.

The oscillations of the vibration drier casing shell are performed under the action of the two unbalance vibration exciters generating centrifugal inertial forces, the vertical components of which act as the perturbing forces in the said oscillations.

The equivalent schematic model features the following forces:

$\bar{F}_{b1}, \bar{F}_{b2}$  – perturbing forces of the forced translational oscillations of the vibration drier casing shell (vertical components of the centrifugal inertial forces generated by the rotation of the vibration exciter eccentric weights and applied at the points  $M_1$  and  $M_2$ , respectively);

$\bar{P}_1, \bar{P}_2$  – elastic forces generated by the longitudinal deformation of the vertical springs  $A_1B_1$  and  $A_2B_2$  and applied at the points  $B_1$  and  $B_2$ , respectively;

$\bar{T}_i$  ( $i = \overline{1,4}$ ) – elastic forces generated by the longitudinal deformation of the horizontal springs  $D_iL_i$  ( $i = \overline{1,4}$ ) and applied at the points  $D_i$  ( $i = \overline{1,4}$ ), respectively;

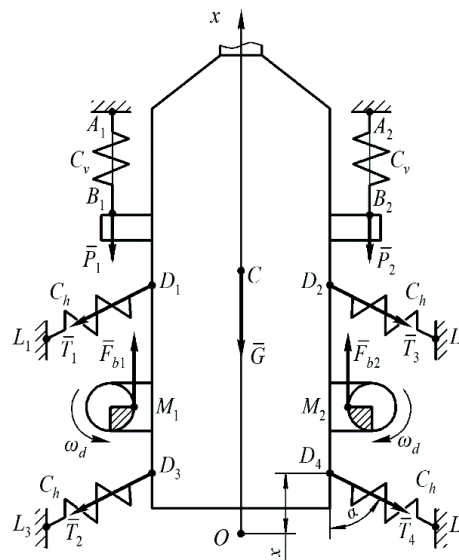


**Figure 2.** Equivalent schematic model of oscillations performed by vibration drier casing shell.

$\bar{G}$  – weight force of the vibration drier casing shell together with the processed food production waste applied at the centre of mass of the vibration drier casing shell (point C).

Fig. 2 also shows the vertical displacement  $x$  of the vibration drier casing shell from its equilibrium position at the random instant of time  $t$ .

Further, it is necessary to determine the magnitudes of all the forces shown in the equivalent schematic model (Fig. 2).

It is obvious that the forces  $F_{bi}$  ( $i = 1, 2$ ) that are the vertical components of the centrifugal inertial forces generated by the rotation of the vibration exciter eccentric weights can be found with the use of the following formula:

$$\bar{F}_{bi} = m_d \cdot r_d \cdot \omega_d \cdot k_d \cdot \cos\left(\omega_d \cdot t\right), (i = 1, 2), \quad (2)$$

where  $m_d$  – mass of the eccentric weight;  $r_d$  – radius of the circle described by the eccentric weight in its rotation;  $\omega_d$  – angular velocity of rotation of the vibration exciter drive shaft;  $k_d$  – number of eccentric weights in the vibration exciter;  $t$  – current time.

In case the revolutions per minute of the eccentric weight are set at  $n_d$ , while the diameter of the circle described by the eccentric weight in its rotation is equal to  $d_d$ , also taking into account that:

$$\omega_d = \frac{\pi \cdot n_d}{30}, \quad (3)$$

the following formula is obtained for finding the magnitudes of the forces  $\bar{F}_{bi}$ :

$$F_{bi} = \frac{\pi^2 \cdot m_d \cdot d_d \cdot n_d^2 \cdot k_d}{1,800} \cdot \cos\left(\frac{\pi \cdot n_d}{30} \cdot t\right), (i = 1, 2), \quad (4)$$

The forces  $P_i$  ( $i = 1, 2$ ) can be determined with the use of the following expression:

$$P_i = C_v \cdot n_{ts} (x + l_{ts}), (i = 1, 2), \quad (5)$$

where  $C_v$  – coefficient of elastic stiffness of the vertical spring;  $n_{ts}$  – number of spring turns in one elastic suspension;  $x$  – amount of the longitudinal deformation of the vertical spring;  $l_{ts}$  – amount of the static longitudinal deformation of the vertical spring.

For the purpose of determining the magnitudes of the elastic forces  $\bar{T}_i$  ( $i = \overline{1, 4}$ ) generated by the horizontal springs, it should be noted that their longitudinal deformations  $l_t$  at the random instant of time  $t$ , are, as can be seen in the equivalent schematic model (Fig. 2), equal to:

$$l_T = \sqrt{x^2 + (l_{hs} + l_{shs})^2} - l_{hs}, \quad (6)$$

where  $l_{hs}$  – design length of the horizontal spring (in its load-free state);  $l_{shs}$  – static deformation of the horizontal spring.

Accordingly, the magnitude of the force  $T_i$  ( $i = \overline{1, 4}$ ) can be determined with the use of the following expression:

$$T_i = C_h \cdot n_{ss} \left( \sqrt{x^2 + (l_{hs} + l_{shs})^2} - l_{hs} \right), (i = \overline{1, 4}), \quad (7)$$

where  $C_h$  – coefficient of elastic stiffness of the horizontal spring;  $n_{ss}$  – number of horizontal springs in one elastic suspension.

At the same time, the vertical components of the forces  $T_i$  ( $i = \overline{1, 4}$ ), that is, their projections on the axis  $Ox$  are equal to:

$$T_i = C_h \cdot n_{ss} \left( \sqrt{x^2 + (l_{hs} + l_{shs})^2} - l_{hs} \right) \cdot \cos \alpha, \quad (i = \overline{1,4}), \quad (8)$$

where  $\alpha$  – angle of inclination of the horizontal springs with respect to the axis  $Ox$  at the random instant of time  $t$  (Fig. 2).

Further, after the  $\cos \alpha$  value is determined and substituted into the expression (8), the following final expression is obtained for the magnitudes of the forces  $T_i$  ( $i = \overline{1,4}$ ) that cause the translational vertical oscillations of the vibration drier casing shell:

$$T_i = C_s \cdot n_{ss} \left( \sqrt{x^2 + (l_{hs} + l_{shs})^2} - l_{hs} \right) \cdot \frac{x}{\sqrt{x^2 + (l_{hs} + l_{shs})^2}}, \quad (i = \overline{1,4}), \quad (9)$$

The force of the weight  $G$  of the vibration drier casing shell together with the process material is equal to:

$$G = m \cdot g, \quad (10)$$

where  $m$  – total mass of the vibration drier casing shell, processed waste and all other vibrating members of the structure;  $g$  – acceleration of gravity.

Further, basing on the generated equivalent schematic model (Fig. 2), the following equation of motion in vector notation can be written for the oscillating vibration drier casing shell together with the processed waste:

$$m\bar{a} = \bar{F}_{b1} + \bar{F}_{b2} + \bar{P}_1 + \bar{P}_2 + \bar{T}_1 + \bar{T}_2 + \bar{T}_3 + \bar{T}_4 + \bar{G}, \quad (11)$$

where  $\bar{a}$  – acceleration of the oscillating casing shell of the vibration drier.

Taking into account the expressions (4), (5), (9) and (10) as well as assuming that the respective forces from different springs are equal to each other, the following differential equation of the oscillations performed by the vibration drier casing shell is derived from the obtained vector Eq. (11) in its projection on the  $Ox$  axis:

$$m\ddot{x} = \frac{\pi^2 \cdot m_d \cdot d_d \cdot n_d^2 \cdot k_d}{900} \cdot \cos\left(\frac{\pi \cdot n_d}{30} \cdot t\right) - 2C_s \cdot n_{ts} (x + l_{ts}) - 4C_s \cdot n_{ss} \left( \sqrt{x^2 + (l_{hs} + l_{shs})^2} - l_{hs} \right) \cdot \frac{x}{\sqrt{x^2 + (l_{hs} + l_{shs})^2}} - mG, \quad (12)$$

from which, after the transformations, the following final expression is obtained:

$$\ddot{x} + \frac{2}{m} \left[ C_s \cdot n_{ts} (x + l_{ts}) + 2C_s \cdot n_{ss} \left( \sqrt{x^2 + (l_{hs} + l_{shs})^2} - l_{hs} \right) \times \right. \\ \left. \times \frac{x}{\sqrt{x^2 + (l_{hs} + l_{shs})^2}} \right] + g = \frac{\pi^2 \cdot m_d \cdot d_d \cdot n_d^2 \cdot k_d}{900m} \cdot \cos\left(\frac{\pi \cdot n_d}{30} \cdot t\right). \quad (13)$$

In order to solve the differential Eq. (13) numerically, it is necessary to specify the design and kinematic parameters of the vibration drier. First of all, the mass parameters have to be defined.

The required parameters of the food production waste drying work process have to be examined and defined. For that purpose, as an example, the initial mass parameters used in a real food production waste processing plant (Sevostianov & Luchik, 2017) are taken under consideration.

First, the total waste mass  $m_o$  has to be determined proceeding from the daily mass  $m_c$  of the food by-products processed in the plant with the use of the vibration drier of the discussed design.  $m_o$  is the mass after the four-stage mechanical dehydration

(Tribuzi & Laurindo, 2014) to a moisture content of  $U_{k.o} = 25\%$ , i.e. the mass of the waste that enters the vibration drier. For the calculation, the following expression is used:

$$m_o = m_c - \frac{U_{n.o} - U_{k.o}}{100} = m_c - m_c \frac{95 - 25}{100} = 0.3 \cdot m_c, \quad (14)$$

where  $U_{n.o} = 95\%$  – initial moisture content in the food by-products.

The total time  $t_z$  spent for feeding the food production waste with a mass of  $m_o$  into the vibration drier under consideration can be found taking into account the production rate  $Q_s$  of the auger feeder with the use of the following formula (Panfilov et al., 2001):

$$t_z = \frac{m_o}{Q_s} = \frac{m_o}{\left[ \frac{m_s \cdot k_s}{4} \cdot (D_s^2 - d_s^2) \right] \cdot \left[ t_s - \frac{b_1 - b_2}{2 \cos \alpha} \right] \cdot n_s \cdot \rho_{o.o} \cdot k_1 \cdot k_2 \cdot k_3}, \quad (15)$$

where  $m_s, k_s, D_s, d_s, t_s, b_1, b_2, \alpha, n_s$  – number of entries in the auger, number of augers, greater and lesser diameters of the auger, pitch of the auger, widths of the helical blade in the cross-section on the inner and outer radii of the auger, angle of helix on the pitch diameter of the auger, rotation speed of the feeder auger, respectively;  $k_1, k_2, k_3$  – coefficients of interturn space filling ( $k_1 = 0.9 - 1.0$ ), waste compression ( $k_2 = 0.51 - 0.56$ ), feeding rate reduction ( $k_3 = 0.9$ ), respectively;  $\rho_{o.o}$  – density of the waste dehydrated to a moisture content of  $U_{k.o} = 25\%$ .

The daily mass  $m_{c.o}$  of the food production waste after drying it to a moisture content of  $U_{c.o} = 8\%$  is calculated as follows:

$$m_{c.o} = m_o - m_o \frac{U_{k.o} - U_{c.o}}{100} = m_o \frac{25 - 8}{100} = 0.17 \cdot m_o = 0.051 \cdot m_c. \quad (16)$$

The time  $t_r$  spent for discharging the food by-products with a mass of  $m_{c.o}$  from the vibration drier can be determined on the basis of the main parameters of the belt conveyor by the formula:

$$t_r = \frac{m_{c.o}}{\rho_{c.o} \cdot v_k \cdot B_k \cdot h_k}, \quad (17)$$

where  $\rho_{c.o}$  – density of waste dehydrated to a moisture content of 8%;  $v_k$  – conveyor belt travel rate;  $B_k$  – working width of conveyor;  $h_k$  – thickness of the dried waste layer on the belt, which corresponds to the clearance between the end face of the slide valve in its open position and the surface of the belt.

Next, it is necessary to operate an experimental prototype of the vibration drier and establish experimentally the time  $t_{s,p}$  spent for drying a batch of food by-products with a mass of  $m_{p,e}$  to a moisture content of  $U_{k.c} = 8\%$ , when the casing shell is filled up and the slide valves are closed.

Taking into account  $t_{s,p}$ , it is possible to find the quantity  $n_p$  of the food production waste batches dehydrated in the unit:

$$n_p = \frac{[24 \cdot 3,600 - (t_z - t_r)]}{t_{c,p}}. \quad (18)$$

The mass  $m_{p,p}$  of one food production waste batch with a moisture content of  $U_{k.o}$ , which the commercial vibration drier must dehydrate in the time  $t_{s,p}$ , can be found with the use of the formula:

$$m_{p,p} = \frac{m_o}{n_p}. \quad (19)$$

The required surface area  $S_{t,p}$  of the heating pipes in the commercial unit is determined with the use of the following relation:

$$S_{t,p} = \frac{m_{p,p}}{m_{p,e}} S_{t,e}, \quad (20)$$

where  $S_{t,e}$  – surface area of the heating pipes in the experimental prototype of the vibration drier.

The length of the heating pipes  $l_t$  is set on the basis of the ceiling height in the shop floor, where the vibration drier is planned to be installed, the height of the auger feeder, the height  $h_n$  of the conical top, the sizes of the clearances  $l_{zv}$ ,  $l_{zn}$ , in accordance with the similar parameters of the experimental prototype, the working length  $l_z$  of the slide valve in its open position, the thickness  $h_k$  of the dried food production waste layer on the belt and the height of the conveyor.

Subsequently, the diameters of the heating pipes  $d_t$  in the middle of the casing shell can be calculated as follows:

$$d_t = \frac{S_{t,p}}{\pi \cdot l_t \cdot n_t}, \quad (21)$$

where  $n_t$  – number of heating pipes.

The height  $h_k$  and radius  $r_k$  of the vibration drier's casing shell is determined by the following formulae:

$$h_k = l_t + l_{zv} + l_{zn}; \quad r_k = \sqrt{\frac{\frac{\pi d_t^2}{4} l_t n_t + \frac{m_{p,p}}{\rho_{o.o}}}{\pi \cdot h_k}}. \quad (22)$$

Knowing the external dimensions of the heating pipes and the casing shell of the vibration drier, their thicknesses are determined following the design considerations; also, taking into account the practice of developing vibration driers (Panfilov et al., 2001), the material for constructing the said components is chosen, after which their masses can be calculated.

Proceeding from the radius  $r_k$  of the vibration drier casing shell and the design considerations, the dimensions and mass  $m$  of the slide valves, with provision for the masses of their attachment units, are determined.

After choosing the electric motors and unbalance vibration exciters, the mass  $m$  is calculated as follows:

$$m = m_{p,p} + m_t + m_k + 2m_z + n_v \cdot m_v + 2m_e + m_{tep}, \quad (23)$$

where  $m_t$ ,  $m_k$ ,  $m_v$ ,  $m_e$  – masses of the heating pipes, casing shell (with provision for the masses of the spring holders), vibration exciter and motor, respectively;  $m_{tep}$  – mass of the heat carrier in the total volume of the heating pipes ( $V_1 = \frac{\pi \cdot d_t^2}{4} l_t \cdot n_t$  – taken into account, when using liquid heat carrier for drying);  $n_v$  – number of vibration exciters.

After that, the horizontal and vertical springs that hold the casing shell in the frame are defined, then the differential Eq. (13) is solved with the use of the PC and numerical techniques.

Proceeding from the obtained results, the criterion that has to be met for the particles in the batch of food production waste in the casing shell to pass in the process

of drying into the vibration-fluidised state is checked in accordance with the expression (1). In case the criterion (1) is not met, the parameters in the Eq. (13) have to be adjusted, then, solving the said equation again, the fulfilment of the criterion (1) has to be achieved.

The primary efficiency parameter of the drying process is the total heat input  $Q$  determined with the use of the methods (Mujumdar, 2014):

$$Q = Q_s + Q_o + Q_{pot}, \quad (24)$$

where  $Q_s, Q_o, Q_{pot}$  – amounts of heat consumed by the drying process itself, the heating of the solid phase of the waste and the heat losses into the ambient environment, respectively. The first term  $Q_s$  can be found with the use of the formula:

$$Q_s = \frac{(m_o - m_{c.o}) \left[ (r_p + c_p T_v) - c_v t_{o1} \right]}{[24 \cdot 3600 - (t_z + t_r)]}. \quad (25)$$

where  $r_p, c_p$  – heat of evaporation and the thermal capacity of vapour, respectively;  $T_v$  – temperature of the air around the drier;  $c_v$  – thermal capacity of water;  $t_{o1}$  – temperature of the waste at the inlet into the drier.

The heat input for heating the solid phase is found as follows:

$$Q_o = \frac{m_{s.o} \cdot c_{s.o} (t_{o2} - t_{o1})}{[24 \cdot 3600 - (t_z + t_r)]}, \quad (26)$$

where  $c_{s.o}$  – specific thermal capacity of dried waste;  $t_{o2}$  – final temperature of the waste approximately equal to the temperature  $T_T$  of the heat carrier in the heating pipes.

The last term in the formula (24) can be presented, in accordance with the results of experimental research found in (Sevostianov & Luchik, 2017), in the form of the following relation:

$$Q_{pot} = 0.1 \cdot Q_s, \quad (27)$$

When the value  $Q$  is known, it is possible to calculate the required heat-transfer surface area  $S_{t.p.n}$  of the heating pipes:

$$S_{t.p.n} = \frac{Q}{K_p (T_T - t_{o1})}, \quad (28)$$

where  $K_p$  – heat transfer coefficient (kinetic coefficient).

Thus, in order to ensure the efficient operation of the unit, the surface area  $S_{t.p}$  of its heating pipes that corresponds to the targeted work process productivity (see the expression 20) has to be equal to or greater than the heat exchange surface area  $S_{t.p.n}$  (see the expression 28):

$$S_{t.p} \geq S_{t.p.n}, \quad (29)$$

The required surface area  $S_{t.p}$  of the heating pipes in the industrial vibration drier unit is determined in accordance with the expression (20). Obviously, it must be equal to or greater than the heat exchange surface area  $S_{t.p.n}$  of the heating pipes.

That said, in case the criterion (29) is not met, the parameters  $n_t, r_t$  have to be selected in accordance with the heat-transfer surface area  $S_{t.p.n}$  and the length  $l_t$  of the heating pipes.

Also, the value  $Q$  provides the basis for calculating the required mass  $G_{t,t}$  of the heat carrier supplied into the heating pipes:

$$G_{t,t} = \frac{Q}{c_p (T_T - t_{o1})}, \quad (30)$$

which then can be compared with the actual mass  $G_t$ :

$$G_t = n_t \cdot \pi \cdot r_t^2 \cdot l_t \cdot \rho_t \geq G_{t,t}, \quad (31)$$

where  $\rho_t$  – specific gravity of the heat carrier in the heating pipes.

When the mode of operation of the plant is the continuous drying of food production waste, the mean rate of travel  $v_o$  of the waste in the vibration drier casing shell is found, taking into account the specified daily output of the proposed equipment, as follows:

$$v_o = \frac{m_o}{24 \cdot 3,600 \cdot \rho_{o,o} \cdot S_p}, \quad (32)$$

where  $S_p$  – passage area of the auger feeder.

Then, the required area  $S_z$  of the passage in the slide valves is equal to:

$$S_z = \frac{m_o}{\rho_{o,o} \cdot v_o}. \quad (33)$$

## RESULTS AND DISCUSSIONS

The heat input required for implementing the drying work process in the continuous mode of operation is determined by the formulae (24–27).

The next task is to calculate the relations between  $S_{t,p,n}$  and varying  $K_p$  and  $t_{o2}$ , then to calculate and plot the relations between the principal design parameters of the pipes, i.e.  $r_t$ ,  $l_t$ ,  $n_t$ , at the fixed minimum values of  $S_{t,p,n}$  and  $G_{t,t}$ . In the calculation, the formulae (14–17, 24–28) have been used together with the following initial parameters (see above):  $m_s = 10,000$  kg;  $r_s = 0.4$  m;  $D_s = 0.8$  m;  $d_s = 0.7$  m;  $n_s = 0.01$  s<sup>-1</sup>;  $t_s = 0.25$  m;  $\rho_{o,o} = 950$  kg·m<sup>-3</sup>;  $\rho_{s,o} = 162$  kg m<sup>-3</sup>;  $m_s = 1$ ;  $k_s = 2$ ;  $b_1 = 0.02$  m;  $b_2 = 0.025$  m;  $\alpha = 6.3^\circ$ ;  $k_1 = 0.95$ ;  $k_2 = 0.52$ ;  $k_3 = 0.9$ ;  $r_p = 2,258$  kJ g<sup>-1</sup>;  $c_p = 2,135$  J kg<sup>-1</sup> K<sup>-1</sup>;  $c_v = 1,877$  J kg<sup>-1</sup> K<sup>-1</sup>;  $t_{o1} = 20$  °C;  $T_v = 20$  °C;  $c_{s,o} = 1,100$  J kg<sup>-1</sup> K<sup>-1</sup>;  $v_k = 1$  m s<sup>-1</sup>;  $B_k = 1.5$  m;  $h_k = 0.1$  m;  $t_{o2} = 50$ – $100$  °C;  $K_p = 10$ – $60$ ;  $n_t = 50$ – $200$ ;  $l_t = 1$ – $5$  m;  $r_t = 0.025$ – $0.1$  m.

For the purpose of PC-assisted calculation, a programme has been compiled in the Microsoft Excel 2016 environment, with the use of which the initial data for plotting the graphical relations have been obtained.

The data calculated with the use of the PC for plotting the relation between the heat transfer area  $S_{t,p,n}$  and the temperature  $t_{o2}$  were first used together with the expression (28) for generating Table 1, which contained the initial data of the said relation at a fixed value of  $K_p = 10$ , i.e. at its minimum value.

After that, the numerical values presented in Table 1 were used for

**Table 1.** Heat transfer surface area of heating pipes in relation to final temperature of dried waste

| $t_{o2}$ , °C                | 50   | 60   | 70   | 80   | 90   | 100  |
|------------------------------|------|------|------|------|------|------|
| $S_{t,p,n}$ , m <sup>2</sup> | 2.57 | 2.22 | 2.01 | 1.87 | 1.77 | 1.69 |

plotting the diagram shown in Fig. 3, which represented the relation between the heat transfer area  $S_{t.p.n}$  and the temperature  $t_{o2}$ . In this case, the heat transfer coefficient  $K_p$  with a value of  $K_p = 10$  corresponded to hot air.

The analysis of the graphical relation shown in Fig. 3 proves that for transferring a greater amount of heat to the certain mass of waste by means of heating to a higher temperature  $t_{o2}$ , a smaller heat-transfer surface area  $S_{t.p.n}$  is required. For example, for heating the food by-product to a temperature of  $t_{o2} = 100$  °C, the required heat-transfer surface area  $S_{t.p.n}$  is equal to 1.69 m<sup>2</sup>, which, in case of the specified level of productivity, does not imply increasing the mass and dimension parameters to a higher level, than that of the similar commercial machines used for drying food production waste. The obtained relation (Fig. 3) can be used for comparative analysis in view of the fact that for all the industrial designs of driers represented in reference books and advertising booklets the dimensions of the process chambers are always indicated and that allows to determine easily the respective heat-transfer surface areas (Sazhin, 1984; Ostrikov et al., 2006).

In Fig. 4, the graphical relation between the pipe length  $l_t$  and the pipe radius  $r_t$  is shown. The relation has also been obtained using the expression (28), at fixed values of  $Q$ ,  $T_T \approx 100$  °C,  $t_1$  and the heat transfer coefficient  $K_p$  varying within the range of  $K_p = 10$ –60. As could be expected taking into account the appearance of the expression (28), the graphical relation  $S_{t.p.n} = f(K_p)$  is a decreasing hyperbola, which means that the increase of the coefficient  $K_p$  results in the substantial decrease of the required heat-transfer surface area  $S_{t.p.n}$  of the heating pipes, i.e. the said area depends to a significant extent on the type of heat carrier. Consequently, the dimensions of the vibration drier casing shell can be substantially reduced, which in itself is a very important point. Moreover, the diagram under consideration indicates that a sufficiently high efficiency of the vibration drier can be achieved by using hot air as the heat carrier, because the coefficient of the heat transfer from hot air to the liquid (the moisture evaporated from the waste) is equal to  $K_p = 10$ –60, that is, in case of its minimum guaranteed value of  $K_p = 10$ , the required heat-transfer surface area of the heating pipes

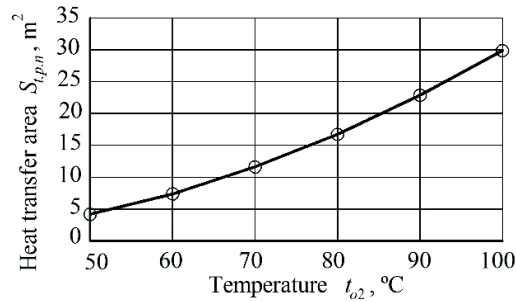


**Figure 3.** Relation between heat-transfer area  $S_{t.p.n}$  and temperature  $t_{o2}$  at  $K_p = 10$ .

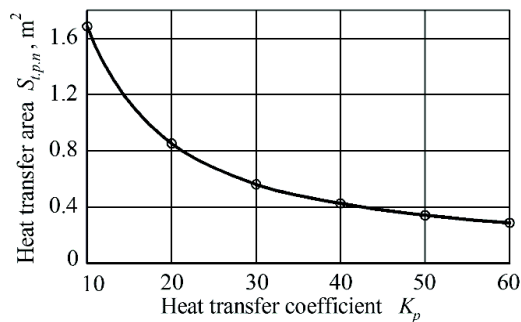


**Figure 4.** Relation between heat-transfer area  $S_{t.p.n}$  and heat-transfer coefficient  $K_p$  at  $t_{o2} = 100$  °C.

amounts to just  $S_{t.p.n} = 1.69 \text{ m}^2$ , which is an acceptable value and can be easily provided in actual practice for a practical vibration drier design.

Thus, it can be stated basing on the relation presented in Fig. 4, the area  $S_{t.p.n}$  and, accordingly, the overall dimensions of the vibration drier casing shell depend to a significant extent on the type of the heat carrier passing in the heating pipes as well as the heat-transfer coefficient  $K_p$  of that heat carrier. That said, the highest efficiency of the vibration drier of the proposed design and its work process is reached in case condensing water steam is used as the heat carrier, as it has  $K_p = 70$  (Mujumdar, A.S. 2014). The obtained graphical relation presented in Fig. 4 can reasonably be used for selecting the most acceptable heat carrier on the basis of the available workspace for installation of the unit.

The application of the obtained expression (21) has provided for plotting the graphical relation between the length of pipe  $l_t$  and the radius of pipe  $r_t$ . For that purpose, the expression (21) has been transformed into the functional relation of the following form:  $l_t = S_{t.p.n} \cdot (2\pi \cdot r_t \cdot n_t)^{-1}$ . The graph of the function  $l_t = f(r_t)$  at fixed values of  $S_{t.p.n}$ ,  $K_p = 30$  (i.e. its mean value),  $t_{o2} = 70 \text{ }^\circ\text{C}$ , the number of pipes  $n_t$  and the increasing value of the pipe radius  $r_t$  is a decreasing hyperbola, as can be seen in Fig. 5.

As is obvious from the diagram shown in Fig. 5, at a fixed number of pipes of  $n_t = 7$ , which can be assumed acceptable in terms of the dimensions and the manufacturing complexity, when the radius  $r_t$  of the pipes increases from 0.025 to 0.060 m, their required length  $l_t$  becomes significantly reduced. In that context, values of  $l_t = 5\text{--}10 \text{ m}$  acceptable for the majority of plants in the food industry are reached at  $r_t \approx 0.055\text{--}0.08 \text{ m}$ . The relation presented in Fig. 5 can be used in designing the unit on the basis of the pipe grades already available at the manufacturing plant or in order to achieve the conformance of the  $r_t$  value to the actual pipe cross-section in the already operated equipment (conformance to the company's internal standards).

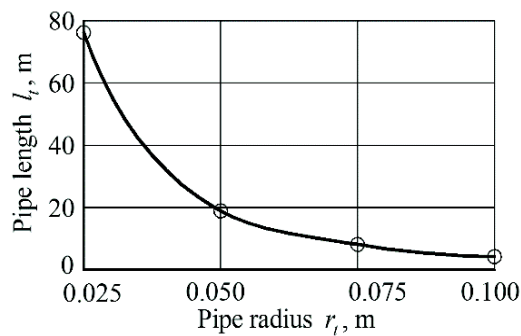


**Figure 5.** Relation between length of pipe  $l_t$  and its radius  $r_t$  at:  $t_{o2} = 70 \text{ }^\circ\text{C}$ ;  $n_t = 7$ ;  $K_p = 30$ .

The diagram that shows the relation between the pipe radius  $r_t$  and the number of pipes  $n_t$  presented in Fig. 6 has been obtained with the use of the expression (21) at fixed values of  $S_{t.p.n}$ ,  $K_p = 30$ ,  $t_{o2} = 70 \text{ }^\circ\text{C}$ , the length of pipe  $l_t = 5 \text{ m}$  and the number of pipes varying within the range of  $n_t = 4\text{--}20$  pieces. As is obvious from the expression (21), it is also a decreasing hyperbola.

The analysis of the graphical relation diagram presented in Fig. 6 shows that, in case of a value of  $l_t = 5$  m, which is acceptable in the majority of cases, when the number of pipes  $n_t$  varies within the range from 4 to 20, the radius of pipe  $r_t$  stays within an acceptable range:  $r_t = 0.046\text{--}0.103$  m. The diagrams in Fig. 5 and 6 give evidence of the fact that the length of pipe  $l_t$  has a greater impact on the required radius of pipe  $r_t$ , than the number of pipes  $n_t$ . The same as in case of the preceding graph, the relation shown in Fig. 6 can be used for the comparative analysis of several the unit design versions on the basis of the available pipe sizes in order to select the optimum solution.

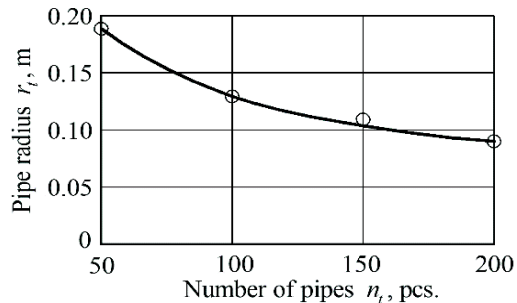


**Figure 6.** Relation between radius of pipe  $r_t$  and number of pipes  $n_t$  at:  $l_t = 5$  m;  $K_p = 30$ ;  $t_{o2} = 70$  °C.

The graph that shows the relation between the number of pipes  $n_t$  and the length of pipe  $l_t$  presented in Fig. 7 has also been obtained with the use of the expression (21), at fixed values of  $S_{t.p.n}$ ,  $K_p = 30$ ,  $t_{o2} = 70$  °C, the radius of pipe  $r_t = 0.05$  m and the length of pipe  $l_t$  varying within the range of  $l_t = 1\text{--}5$  m. The curve of the relation is, again, a decreasing hyperbola.

The obtained graphical relation indicates that, if the radius of pipe is constant:  $r_t = 0.1$  m, the increase of the value  $l_t$  from 1 to 5 m (Fig. 7) results in the decrease of the number of heat-exchange pipes  $n_t$  to a level within the acceptable value of 200 pieces for the length of pipes within  $l_t = 4.4\text{--}5.0$  m, that is, to the value, at which it is possible to select the principal design parameters of the pipes and, accordingly, the overall dimensions of the drier's casing.

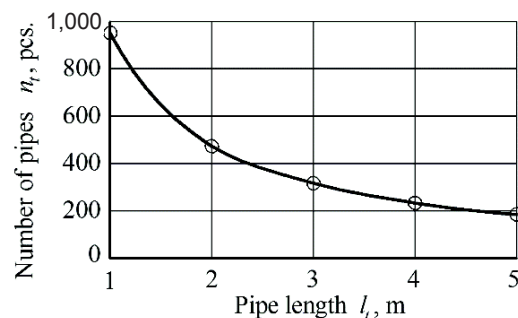


**Figure 7.** Relation between number of pipes  $n_t$  and length of pipe  $l_t$  at:  $r_t = 0.05$  m;  $K_p = 30$ ;  $t_{o2} = 70$  °C.

Thus, the relation presented in Fig. 7 allows calculating the principal design parameters of the drying unit on the basis of the ceiling height in the shop, where the unit is to be installed and operated in the future.

In accordance with the diagrams shown in Fig. 5–7, the reasonable design and process parameters of the vibration drier type under consideration in terms of achieving the specified work process productivity and final moisture content in the dehydrated food production waste are as follows:  $r_t = 0.05\text{--}0.10$  m;  $l_t = 3.0\text{--}5.0$  m;  $n_t = 7\text{--}20$ , at  $K_p = 30\text{--}60$  and  $t_{o2} = 60\text{--}80$  °C.

In general, the obtained relations can be used as the basis for developing a computer-aided engineering technique for the design calculation of the proposed vibration drier.

## CONCLUSIONS

1. The analysis completed by the authors has revealed that the air-fluidised and vibration-fluidised bed units are the most suitable equipment for food production waste drying. In comparison with other types of equipment for similar applications, these units ensure high productivity and energy efficiency, while having a simpler and more reliable design.

2. At the same time, the analysis has shown that the known designs of vibration driers are rather bulky and reducing their energy intensity also remains the order of the day.

3. The authors have proposed the improved design of the vibration drier, in which the heat energy output from the primary production work of the plant is utilised, which provides for bringing down the energy intensity of the drying process to a minimum as compared to the drying installations that operate with the use of organic fuels or electric power for heating. Moreover, the design of the drier eliminates the possibility of clogging the passage spaces, where the waste and heat carrier flow. The number of auxiliary components, dimensions and cost have been reduced as compared to the known equipment.

4. The equivalent schematic model of the forces acting on the casing shell of the vibration drier has been developed and on its basis the differential equation of the translational vertical oscillations of the casing shell together with the processed food production waste has been generated. The PC-assisted solving of the above-mentioned equation allows to determine the needed conditions of the vibratory fluidisation of the processed material.

5. The relations have been proposed for determining the main efficiency parameters of the developed new vibration drier - the required heat energy consumption rate  $Q$  proceeding from the specified and chosen physical and mechanical properties of the processed waste and design parameters of the equipment.

6. On the basis of the above-mentioned relations, the computer programme for calculation has been compiled and with its use the diagrams have been obtained for selecting the reasonable parameters of the drier and ensuring the specified work process productivity and final moisture content in the food production waste, without needing any additional heat input. The obtained relations can be used in the further theoretical and experimental investigations on the drier as well as the development of the technique for its design calculation.

## REFERENCES

- Aboltins, A. & Upitis, A. 2012. Experimental and theoretical investigation of agricultural material drying process. *Engineering for Rural Development* **11**, 93–98.
- Atkinson, B. 1979. *Biochemistry reactors*. Moskow, Food Processing Industry, 280 pp. (in Russian)
- Atkinson, B. & Mavituna, F. 1991. *Biochemical Engineering and Biotechnology Handbook*. 2nd Edition, Stockton Press, 1271 pp.
- Altieri, G. 2020. Comparative trials and an empirical model to assess throughput indices in olive oil extraction by decanter centrifuge. *Journal of Food Engineering* **97**(1), 46–56. doi: 10.1016/j.jfoodeng.2009.09.014

- Antal, T., Kerekes, B., Sikolya, L. & Tarek, M. 2015. Quality and Drying Characteristics of Apple Cubes Subjected to Combined Drying (FD Pre-Drying and HAD Finish-Drying). *Journal of Food Processing and Preservation* **39**(6), 994–1005. doi: 10.1111/jfpp.12313
- Beránek, L. & Kolařík, K. 2014. Surface integrity analysis of duplex steel by design of experiment Approach. *Procedia Engineering* **69**, 630–637. doi: 10.1016/j.proeng.2014.03.036
- Bezbakh, I.V. & Bakhmutyan, N.V. 2006. Investigation of the drying process of fruits and berries in a suspended layer. *Scientific works of ONAHT*, Odessa, **28**, pp. 112–116.
- Boyce, D.S. 1965. Grain moisture and temperature changes with position and time during through drying. *Journal of Agricultural Engineering Research* **10**(4), 333–341. doi: 10.1016/0021-8634(65)90080-6
- Bruce, D.M. & Giner, S.A. 1993. Mathematical modelling of grain drying counter-flow beds: Investigation of crossover of air and grain temperatures. *Journal of Agricultural Engineering Research* **55**(2), 143–161. doi: 10.1006/jaer.1993.1039
- Bulgakov, V., Bandura, V., Arak, M. & Olt, J. 2018. Intensification of rapeseed drying process through the use of infrared emitters. *Agronomy Research* **16**(2), 349–356. doi: 10.15159/AR.18.054
- Bulgakov, V., Holovach, I., Kiurchev, S., Pascuzzi, S., Arak, M., Santoro, F., Anifantis A.S. & Olt, J. 2020. The theory of vibrational wave movement in drying grain mixture. *Agronomy Research* **18**(2), 360–375. doi: 10.15159/AR.20.051
- Daud, W.R.W. 2008. Fluidized Bed Dryers – Recent Advances. *Advanced Powder Technology* **19**(5), 408–418. doi: 10.1163/156855208X336675
- Dufour, P. 2006. Control engineering in drying technology: Review and trends. *Drying Technology* **24**(7), 889–904. doi: 10.1080/07373930600734075
- El Hor, H., Linz, S.J., Grochowski, R., Walzel, P., Kruelle, C.A., Rouijaa, M., Götzendorfer, A. & Rehberg, I. 2005. Model for transport of granular matter on vibratory conveyors. *Powders and Grains 2005 - Proceedings of the 5th International Conference on Micromechanics of Granular Media* **2**, 1191–1195.
- Filonenko, G.K. & Grishin, M.A. 1971. *Drying of food plant materials*. Moscow, Food Processing Industry, 231 pp. (in Russian)
- Giner, S.A. 2019. Estimation of the influence of variable boundary when using thin layer equations for grain dryer simulation. *Biosystems Engineering* **186**, 228–233. doi: 10.1016/j.biosystemseng.2019.08.004
- Goncharevich, I.F., Uriev, I.B. & Taleysnik, M.A. 1977. *Vibration engineering in food industry*. Moscow: Food Industry, 279 pp. (in Russian).
- Handayani, S.U, Utomo, Tony Suryo Utomo, M.S.K. & Yulianto, M.E. 2017. Performance evaluation of continuous vibrating fluidized bed dryer on green tea production. *Advanced Science Letters* **23**(3), 2530–2532. doi: 10.1166/asl.2017.8676
- Hemis, M., Choudhary, R. & Watson, D.G. 2012. A coupled mathematical model for simultaneous microwave and convective drying of wheat seeds. *Biosystems Engineering* **112**(3), 202–209. doi: 10.1016/j.biosystemseng.2012.04.002
- Hoffman, P., Pěnička, M. & Fořt, I. 2017. Effect of Fluidized Bed Stirring on Drying Process of Adhesive Particles. *Chemical and Biochemical Engineering Quarterly* **31**(1), 1–10. doi: 10.15255/CABEQ.2015.2335
- Kliuchnikov, A. 2019. Development of new method of drying at energy-saving universal dryer to improve quality of crops used in fodder production. *Engineering for Rural Development* **18**, 105–111. doi: 10.22616/ERDev2019.18.N125
- Lehmann, S.E., Hartge, E.-U., Jongasma, A., deLeeuw, I.-M., Innings, F. & Heinrich, S. 2019. Fluidization characteristics of cohesive powders in vibrated fluidized bed drying at low vibration frequencies. *Powder Technology* **357**, 54–63. doi: 10.1016/j.powtec.2019.08.105

- Ma, J., Zhang, L., Mu, L., Zhu, K. & Li, A. 2018. Thermally assisted bio-drying of food waste: Synergistic enhancement and energetic evaluation. *Waste Management* **80**, 327-338. doi: 10.1016/j.wasman.2018.09.023
- McKenna, J.V. 1986. Centrifuging citrus waste & juice. *Transactions of the Citrus Engineering Conference* **32**, 49–64. doi: 10.1115/cec1986-3205
- Mohseni, M., Kolomijtschuk, A., Peters, B. & Demoulling, M. 2019. Biomass drying in a vibrating fluidized bed dryer with a Lagrangian-Eulerian approach. *International Journal of Thermal Sciences* **138**, 219–234, doi: 10.1016/j.ijthermalsci.2018.12.038
- Mujumdar, A.S. 2014. *Handbook of Industrial Drying*, 4th Edition, CRC Press, 1348 p, eISBN: 9780429169762. doi: 10.1201/b17208
- Ostrikov, A.N., Krasnovitskiy, J.V. & Petrov, S.M. 2006. *Processes and apparatus for food production*. Book 2, St. Petersburg: GIORD, 559 pp.
- Ovchinnikov, N.L., Ovchinnikov, L.N. & Natareev, S.V. 2009. *Drying and baking in fluidized bed*. Ivanovo: GOUVPO Ivanov State Chemical Engineering University, 106 pp.
- Palamarchuk, I.P., Kurchev, S.V. & Verkholtantseva, V.A. 2018. Trends in the development of conveyor vibratory dryers. In: *The development of technical sciences: problems and solutions: Proceedings of the international research and practical conference (April, 27–28, 2018)*, Brno, pp. 9–12.
- Panfilov, V.A., Antipov, S.T., Kretov, I.T. & Ostrikov, A.N. 2001. *Technique and apparatus for food industry*. Moscow, Higher School, 703 pp. (in Russian)
- Robaina-Mesa, M. & Chanfrau, J.E.R. 2019. Spray drying of pectin obtained from citrus sinensis waste. *Biointerface Research in Applied Chemistry* **10**(1), 4825–4828. doi: 10.33263/BRIAC101.825829
- Ruiz Celma, A., Cuadros, F. & López-Rodríguez, F. 2012. Characterization of pellets from industrial tomato residues. *Food and Bioproducts Processing* **90**(4), 700–706, doi: 10.1016/j.fbp.2012.01.007
- Sazhin, B.S. 1984. *Foundations of the theory of drying*. Moscow, Chemistry, 320 pp.
- Sevostianov, I.V. 2013. *Processes and equipment for vibro-blowing separation of food waste*, Saarbrücken: LAP LAMBERT Academic Publishing, 417 pp, ISBN: 978-3-659-47395-1.
- Sevostianov, I.V., Polischuck, O.V. & Slabkiy, A.V. 2015. Elaboration and research of an installation for two-component vibro-blowing dehydration of waste food productions. *Eastern-European Journal of Enterprise Technologies* **5**(7), 40–46, doi: 10.15587/1729-4061.2015.49272
- Sevostianov, I.V. & Luchik, V.L. 2017. Installation for multi-stage dehydration of food production waste. *Mechanical Engineering and Transport News* **1**, 105–113 (in Russian).
- Tribuzi, G. & Laurindo, J.B. 2014. How to Adapt a Lab-Scale Freeze Dryer for Assessing Dehydrating Curves at Different Heating Conditions. *Drying Technology* **32**(9), 1119–1124. doi: 10.1080/07373937.2014.886258
- Wawrzyniak, P., Jaskulski, M., Piatkowski, M., Sobulska, M., Zbicinski, I. & Egan, S. 2020. Experimental detergent drying analysis in a counter-current spray dryer with swirling air flow. *Drying Technology* **38**(1–2), 108–116. doi: 10.1080/07373937.2019.1626878
- Wang, X., Zhang, Z. & Deng, Y. 2011. The harmonic response analysis on vibration system of disc vibration dryer. *Applied Mechanics and Materials* **84–85**, 209–213. doi: 10.4028/www.scientific.net/AMM.84-85.209
- Ward, K. 2002. Drying out: Technology comes in from the cold. *Chemical Engineer* **734**, 26–27.
- Yogendrasidhar, D. & Setty, Y.P. 2019. Experimental studies and thin layer modeling of pearl millet using continuous multistage fluidized bed dryer staged externally. *Engineering Science and Technology, an International Journal* **22**(2), 428–438. doi: 10.1016/j.jestch.2018.10.010